



Published in final edited form as:

Mol Imaging. 2013 June 1; 12(4): 244–256.

Measuring Response to Therapy by Near-Infrared Imaging of Tumors Using a Phosphatidylserine-Targeting Antibody Fragment

Jian Gong, Richard Archer, Michael Brown, Seth Fisher, Connie Chang, Matthew Peacock, Christopher C.W. Hughes, and Bruce Freimark

Departments of Preclinical Development, Oncology, and Process Sciences, Peregrine Pharmaceuticals, Inc., Tustin, CA, and the Department of Molecular Biology and Biochemistry, University of California, Irvine, CA

Abstract

Imaging tumors and their response to treatment could be a valuable biomarker toward early assessment of therapy in patients with cancer. Phosphatidylserine (PS) is confined to the inner leaflet of the plasma membrane in normal cells but is externalized on tumor vascular endothelial cells (ECs) and tumor cells, and PS exposure is further enhanced in response to radiation and chemotherapy. In the present study, we evaluated the potential of a PS-targeting human F(ab')₂ antibody fragment, PGN650, to detect exposure of PS in tumor-bearing mice. Tumor uptake of PGN650 was measured by near-infrared optical imaging in human tumor xenografts in immunodeficient mice. PGN650 specifically targeted tumors and was shown to target CD31-positive ECs and tumor cells. Tumor uptake of PGN650 was significantly higher in animals pretreated with docetaxel. The peak tumor to normal tissue (T/N) ratio of probe was observed at 24 hours postinjection of probe, and tumor binding was detected for at least 120 hours. In repeat dose studies, PGN650 uptake in tumors was significantly higher following pretreatment with docetaxel compared to baseline uptake prior to treatment. PGN650 may be a useful probe to detect PS exposed in tumors and to monitor enhanced PS exposure to optimize therapeutic agents to treat tumors.

Detection of tumors at early stages is critical for effective treatment of cancer and monitoring response to therapy.^{1,2} Imaging technology to detect molecular changes in the asymmetry of phospholipid distribution in the cell membrane bilayer is a growing field of preclinical and clinical research to detect tumors and measure responses to therapy.³ Phosphatidylserine (PS) is the most abundant anionic aminophospholipid present in the cell membrane of all mammalian cells and is located in the inner leaflet of the cell membrane of

© 2013 Decker Publishing

Address reprint requests to: Bruce Freimark, PhD, Department of Preclinical Development, Oncology, Peregrine Pharmaceuticals, Inc., 14282 Franklin Avenue, Tustin, CA 92780; bfreimark@peregrineinc.com..

Financial disclosure of authors: Christopher C.W. Hughes is professor and chair of the Department of Molecular Biology and Biochemistry, UCI, and is a consultant to Peregrine Pharmaceuticals. He is supported by award number P30 CA062203 from the National Cancer Institute. M. Peacock is a research scientist working in the laboratory of Christopher C.W. Hughes. All other authors are employees of Peregrine Pharmaceuticals.

Financial disclosure of reviewers: None reported.

normal, healthy cells.⁴ This asymmetry of PS is mediated by two adenosine triphosphate (ATP)-dependent translocase enzymes, and externalization is the result of translocase inactivation and activation of an ATP-independent scramblase.⁵ PS exposure is evident on external cell membranes of viable cells undergoing cellular stress, dying or apoptotic cells, and necrotic cells, where the integrity of the cell membrane is lost, allowing exposure of the inner leaflet. PS is exposed on the surface of tumor vascular endothelium, in response to stress conditions such as hypoxia, acidity, thrombin, inflammatory cytokines, and reactive oxygen species in the tumor microenvironment.^{6,7} Evidence that tumor vascular endothelial cells (ECs) are viable and not apoptotic or necrotic includes the following: (1) they lack active caspase-3 and are TUNEL negative, (2) they can produce rapidly turned-over proteins such as vascular cell adhesion molecule 1 (VCAM-1), and (3) they allow perfusion of blood, which allows access of intravenously administered therapeutic agents and imaging agents.⁶⁻⁸

Detection of PS exposure through histologic techniques is limited by several factors, including the heterogeneity of tumor sampling and the lack of surgical accessibility of some tumors. In addition, histologic sectioning of tissues disrupts cell membranes and may artifactually expose PS on the inner leaflet of healthy cells, which would confound the accurate identification of disease tissue. Thus, development of noninvasive imaging methods to detect PS exposure would permit the accurate identification of lesions. Detection of PS exposure has been reported by both radionuclide and nonradionuclide imaging methods with a variety of PS-binding reagents, including proteins,⁹ peptides,^{10,11} and small-molecular-weight compounds.^{12,13} Annexin V is the most widely used protein to visualize PS exposure in cancer patients by nuclear imaging techniques, with ^{99m}Tc being the most common radionuclide used for single-photon emission computed tomography (SPECT).¹⁴ However, annexin V has a free circulating half-life of 3 to 7 minutes when injected intravenously and targets normal kidney tissue, which may limit its use for clinical imaging and measuring peak probe uptake responses to therapy.^{15,16}

Monoclonal antibodies have been generated that target PS exposure on tumor vasculature endothelium, and localization has been demonstrated in several rodent tumor models.^{6,8,17} Antibody 3G4, a murine IgG3 monoclonal antibody, binds PS through the interaction of 3G4 with the PS-binding plasma protein β_2 -glycoprotein 1 (β_2 GP1)¹⁸ and stabilizes a complex of two molecules of β_2 GP1 bound to PS on the cell surface.¹⁹ The affinity for the binding of the antibody- β_2 GP1 complex to PS is extremely strong—on the order of dissociation constant (K_d) \approx 1 nM. Bavituximab, currently in several phase II clinical trials for solid tumors, including non-small cell lung and pancreatic cancer, is a human-mouse chimeric antibody, with variable regions from antibody 3G4 fused to human IgG1 κ constant regions.²⁰ Using a rat prostate tumor model, bavituximab radiolabeled with ⁷⁴As has been successfully used as a positron emission tomographic (PET) probe to image tumors.²¹

PGN635 is a fully human antibody that also targets PS through the interaction of β_2 GP1 with an affinity for PS- β_2 GP1 complexes similar to 3G4 and bavituximab.²² Recently, using near-infrared (NIR) optical imaging, the use of a F(ab')₂ fragment of PGN635 labeled with the NIR fluorescent dye IRDye 800CW, designated as 800CW-PGN650, was used to demonstrate tumor uptake in a model of rat glioma and enhancement of probe uptake by irradiation of tumors.²³ In this study, we sought to explore the use of 800CW-PGN650 as an

imaging agent to monitor the exposure of PS in tumors and to assess responses to chemotherapy. Measurement of PS exposure in response to chemotherapy was assessed using human breast and prostate tumor xenografts in mice. In both tumor models, elevated levels of PS were detected in tumors following administration of docetaxel, which was confirmed by ex vivo imaging of tumors and fluorescence microscopy. Additionally, 800CW-PGN650 was used to establish a baseline uptake of probe in tumors, which was compared to uptake of probe following chemotherapy. Our observations indicate that PGN650 has the potential to be used as an imaging agent to detect tumors and measure the response to chemotherapeutic agents.

Materials and Methods

Preparation of NIR F(ab')₂ Fragments

The human monoclonal antibody PGN635 (also known as 1N11) is an IgG1 λ generated by Affitech A.S. (Oslo, Norway) in collaboration with Peregrine Pharmaceuticals, Inc. (Tustin, CA). PGN635 targets PS in the presence of circulating protein β 2GP1 of multiple species, including bovine, murine, rat, monkey, and human. A human IgG1 monoclonal antibody binding a hepatitis C viral protein was used as a negative control antibody (cIgG). Both antibodies were produced under serum-free conditions by Avid Bioservices (Tustin, CA). F(ab')₂ fragments of PGN635 and cIgG were generated by digestion with pepsin at a 1:40 pepsin:antibody (w:w) in 100 mM acetate buffer, pH 3.6, for 0.5 hours at 37°C. F(ab')₂ fragments were purified by cation exchange chromatography and affinity chromatography followed by anion exchange chromatography to remove pepsin and Fc fragments. The material was then concentrated and formulated in acetate buffer, pH 5.0. The PGN635 F(ab')₂ fragment is designated PGN650. F(ab')₂ fragments were incubated with IRDye 800CW (Li-COR, Lincoln, NE) at a molar ratio of 1:10 (protein:dye) for 2 hours at room temperature. Unreacted dye was separated from the conjugate by dialysis against phosphate-buffered saline (PBS) buffer. Fluorescent conjugates labeled with IRDye 800CW display an absorption maximum of 774 nm and an emission maximum of 789 nm in 1 \times PBS. Analyses of the final product, based on the absorbance of the dye at 778 nm and the absorbance of the F(ab')₂ protein at 280 nm, showed that it consisted of approximately one to two molecules of dye bound to each F(ab')₂ fragment. The binding activity of 800CW labeled and unlabeled PGN650 was compared using an enzyme-linked immunosorbent assay (ELISA) method. The labeled F(ab')₂ fragments were tested for endotoxin prior to dosing in animals. The labeled F(ab')₂ fragments were referred to as 800CW-PGN650 or 800CW-cIgG F(ab')₂ throughout the study.

Targeting of PGN650 to Immobilized PS and Cell Surfaces

PGN650 targeting to PS was performed by a solid-phase ELISA and cell-based flow cytometry in the presence of serum as a source of β 2GP1 using a modification of a previously described method.²⁴ For the ELISA, PS was diluted in hexane and dispensed into the wells of a 96-well microtiter plate. The hexane was allowed to evaporate until dry, leaving the PS coated on the wells. To prevent nonspecific binding, the wells were blocked with 10% (v/v) fetal bovine serum (FBS) in PBS for 2 hours at 37°C and then washed with PBS. The PGN650 or cIgG F(ab')₂ fragments were diluted in blocking buffer and then

serially diluted in the plate to create a dose-response binding curve. The primary antibody, PGN650 or cIgG F(ab')₂, was incubated for 2 hours at 37°C and then washed with PBS. A peroxidase-conjugated secondary antibody specific to human IgG F(ab')₂ was diluted in blocking buffer and then dispensed in the wells and incubated for 1 hour at 37°C. Following a final wash step, wells were developed with tetramethylbenzidine peroxidase substrate solution and quenched with 2 M sulfuric acid, and the absorbance was measured at 450 nm using a microplate spectrophotometer.

Targeting of PGN650 to PS was also performed using a cell-based flow cytometry assay. Jurkat (ATCC, Manassas, VA) tumor cells were cultured for 18 hours in RPMI-1640 containing 10% FBS at 37°C in the presence of 10 µM etoposide to expose cell-surface PS. For blocking studies, etoposide-treated Jurkat cells were incubated for 30 minutes at room temperature with 10 µg PGN650 or cIgG F(ab')₂ in 10% FBS/PBS, in the presence or absence of 10 µg of annexin V (BD Pharmingen, San Diego, CA). Following a wash step, cells were stained with a 1:100 dilution of phosphatidylethanolamine (PE)-labeled antihuman IgG F(ab')₂ antibody for 30 minutes at room temperature, washed, and resuspended in 1% FBS/PBS. Cells were analyzed using a FACSCalibur flow cytometer (BD Biosciences, San Jose, CA).

Tumor Models

All animal procedures were approved by the Institutional Animal Care and Use Committee of the University of California, Irvine (UCI). Human PC-3-luciferase (luc) cells (1×10^6 cells) (obtained from Philip Thorpe, University of Texas Southwestern Medical Center, Dallas, TX) were injected in 50% v/v matrigel (BD Biosciences) subcutaneously in the flank of anesthetized male SCID mice (National Cancer Institute, Frederick, MD). For 800CW-PGN650 and 800CW-cIgG F(ab')₂ dose titration studies, 24 animals were injected and separated into 3 animals per group. For studies to examine 800CW-PGN650 uptake in response to chemotherapy, 16 SCID mice were injected with tumors and separated into groups of 4 animals per group. Human BT474 breast tumors (ATCC) were established by injecting 1×10^7 cells in 200 µL serum-free medium containing 50% (v/v) Matrigel, orthotopically under the left inguinal nipple of anesthetized nude female BALB/c nu/nu mice (Harlan, Indianapolis, IN) implanted subcutaneously with a 1.5 mg, 60-day release β-estradiol pellet (Innovative Research, Sarasota, FL). For studies to examine 800CW-PGN650 uptake in response to chemotherapy, 12 nude mice were injected with tumors and separated into groups of 3. All tumors were allowed to grow to 200 to 500 mm³ prior to initiation of chemotherapy and imaging.

NIR Fluorescence and Bioluminescent Imaging

NIR fluorescence imaging and bioluminescent imaging (BLI) was performed using a Lumina II imaging system (Caliper Life Sciences, Hopkinton, MA). Each mouse was maintained under general anesthesia using a liquid injection mixture of ketamine and xylazine. Images were acquired before and at different times after administration of 800CW-PGN650 or 800CW-cIgG F(ab')₂ via a tail vein injection with varying doses of labeled F(ab')₂ fragments. BLI was detected in animals by subcutaneous injection of 75 mg/kg D-luciferin (Biosynth, USA) 10 minutes prior to imaging. In some studies, docetaxel (Sanofi-

Aventis; obtained from the UCI pharmacy) was administered at 10 mg/kg intraperitoneally (IP) at varying time points prior to injection of 800CW-PGN650. For blocking studies, excess unlabeled PGN650 or cIgG F(ab')₂ was injected 1 hour prior to injection of 800CW-PGN650. Identical imaging parameter settings were used for acquiring all images. Fluorescence images were acquired using 710 nm excitation and 780 nm emission filters and medium binning, F/stop of 4, and exposure time of 3 seconds. BLIs were acquired using medium binning, F/stop of 1, and a 20-second exposure 10 minutes after mice were subcutaneously injected with 75 mg/kg of D-luciferin.

IRDye 800CW carboxylate (Li-COR, Lincoln, NE) was used as a control in animal imaging studies. The carboxylated dye was reconstituted in sterile 1× PBS and filter-sterilized through a 0.2 μm filter before administration. An equal quantity of carboxylated dye to the amount of dye contained in the dose of the IRDye 800CW-labeled antibody was administered to animals intravenously in the studies. Clearance of the carboxylated dye from the animal's body by NIR imaging was about 24 hours (data not shown). Data were analyzed by measuring the photon intensity of the region of interest (ROI) of tumor or normal tissue, and a tumor to normal tissue (T/N) ratio of the NIR signals was determined. Same-size ROI of tumor was gated on mouse leg muscle area as normal tissue for normalization.

Fluorescence Microscopy

Immediately after NIR imaging, mice were sacrificed and tumor tissues were removed and placed in cyromolds containing optimal cutting temperature compound tissue embedding medium, frozen in a dry ice/isobutane bath, and stored at -80°C until cryosections were prepared. Cryosections (5 μM) were immediately immersed in a glyoxal-based fixative (Prefer, Anatech, Battle Creek, MI) at room temperature for 15 minutes to immobilize NIR-labeled F(ab')₂ fragments. Sections were blocked with 10% (w/v) bovine serum albumin (BSA) in PBS for 1 hour at room temperature and incubated with 2.5 μg/mL rat antimouse CD31-Alexa 488 or rat IgG2a-Alexa 488 isotype control (BioLegend, San Diego, CA) diluted in 1% BSA/PBS for 2 hours at room temperature. Tissue sections were washed three times for 5 minutes each at room temperature with PBS, air-dried, and mounted using ProLong Gold containing 4',6-diamidino-2-phenylindole (DAPI) counterstain (Invitrogen, CA). The NIR fluorescent images were detected using a Cy7 filter. Images were captured using a 20× objective on a Nikon E600 microscope equipped with a 150-watt xenon lamp. The NIR, Alexa 488, and DAPI-stained images of the same field were captured and merged, and the integrated NIR signal and overlap with CD31 were determined using *MetaMorph* software (Molecular Devices, Sunnyvale, CA).

Data Processing and Statistics

All data are given as mean ± SEM. Statistical analysis was performed using a Student *t*-test where indicated, with statistical significance assigned for *p* values < .05. Data plotting and statistical analysis were performed using GraphPad *Prism* software version 5.0 (GraphPad Software, La Jolla, CA).

Results

Targeting of PGN650 to PS

Specific targeting of PGN650 to PS coated on the surface of plastic microtiter plates, in the presence of β 2GPI in bovine serum, is observed in a concentration-dependent manner (Figure 1A). In a cell-based fluorescence-activated cell sorting (FACS) assay, PGN650 targets PS exposed on the surface of etoposide-treated Jurkat tumor cells (Figure 1B). Annexin V blocks the binding of 800CW-PGN650, which confirms the targeting to exposed PS. Labeling of PGN650 with 800CW dye does not interfere with the PS targeting activity to cell membranes. The localization and specificity of 800CW-PGN650 binding to tumors were confirmed using a single intravenous dose at 1 mg/kg injected in male SCID mice with human PC-3luc prostate tumors (Figure 1C). Injection of 800CW dye alone is rapidly excreted and is not detected in animals (data not shown). Binding of 800CW-PGN650 to PC-3luc tumors was observed 24 hours following injection, whereas no tumor binding was seen in animals injected with 800CW-cIgG F(ab')₂. Compared to untreated animals, the specific binding of 800CW-PGN650 to PC-3luc tumors was blocked by a 50-fold excess of unlabeled PGN650 but not by the same amount of unlabeled cIgG F(ab')₂ (Figure 1D).

The lower limit of detection of 800CW-PGN650 uptake in tumors was measured in untreated PC-3luc tumor-bearing SCID mice. SCID mice bearing PC-3 tumors were injected intravenously with 800CW-PGN650 or 800CW-cIgG F(ab')₂ at 0.1, 0.3, 1.0, and 3.0 mg/kg, and a T/N ratio of the tumor ROI and normal control tissue was determined at 24, 48, and 96 hours. Compared to 800CW-cIgG F(ab')₂, 800CW-PGN650 binding was observed 24 hours after injection and could be detected for up to 96 hours (Figure 2). The limit of detection of NIR-PGN650 targeting in PC-3 tumors with a single dose was 0.3 mg/kg.

Chemotherapy Enhances Uptake of PGN650 in Tumors

Measurement of tumor response to chemotherapy was conducted in mice with subcutaneous PC-3 prostate tumors or orthotopic human BT-474 breast tumors by injection of 800CW-PGN650 24 hours after treatment with docetaxel. SCID mice bearing PC-3 tumors pretreated with docetaxel (10 mg/kg, IP) 24 hours prior to injection of 800CW-PGN650 (1 mg/kg, IV) had statistically significant enhanced tumor uptake compared to animals pretreated with 0.9% saline for up to 120 hours postinjection (Figure 3). No tumor uptake was observed in animals injected with 800CW-cIgG F(ab')₂ (1 mg/kg, IV) with or without a pretreatment with docetaxel. Similarly, 800CW-PGN650 targeted orthotopic BT-474 breast tumors in docetaxel-treated mice to a greater extent compared to saline-treated animals (Figure 4A). Similar to results with PC-3 tumors, binding of 800CW-PGN650 probe to BT-474 tumors was greater in animals injected with docetaxel (Figure 4B). Some retention of both 800CW-PGN650 and 800CW-cIgG F(ab')₂ was observed in the liver and bladder 24 hours postinjection and was likely due to clearance of the probes through the liver and probe fragments via the kidney and urinary tract. Optical images of BT-474 tumors excised from nude mice injected with 800CW-PGN650 confirmed that tumors from mice treated with docetaxel had higher amounts of antibody compared to tumors from untreated animals (Figure 4C). Excised tumors from animals injected with 800CW-cIgG F(ab')₂ had low levels of binding, and the probe uptake was not affected by pretreatment with docetaxel.

PGN650 Targets Tumor Blood Vessel Endothelium

Quantitation of NIR immunofluorescence signals was conducted on tissue cryosections prepared from BT-474 tumors of mice (shown in Figure 4C) injected with 800CW-PGN650 or 800CW-cIgG F(ab')₂ and treated with or without docetaxel (Figure 5, A and B). The integrated (pixel count × intensity) NIR signals were statistically higher in tumors from animals injected with 800CW-PGN650 compared to tumors from animals injected with 800CW-cIgG F(ab')₂ either with or without pretreatment with docetaxel ($p < .05$). Treatment with docetaxel enhanced the integrated NIR signal 8.4-fold in mice injected with 800CW-PGN650 compared to untreated animals ($p < .05$). 800CW-PGN650 localized to both CD31⁺ positive blood vessel ECs and tumors. Docetaxel induced higher levels of 800CW-PGN650 uptake on CD31⁺ endothelial cells (merged yellow color); however, the percent overlap of NIR signal with CD31 staining did not significantly change in mice treated with or without docetaxel. Minimal staining was observed in tumors from animals injected with 800CW-cIgG F(ab')₂.

Repeat Administration of PGN650 to Measure Tumor Uptake Before and After Chemotherapy

Establishing the feasibility of determining the baseline tumor uptake of PGN650 and then measuring the peak tumor uptake after administration of chemotherapy in the same animal is an important step prior to conducting similar studies in patients. To address this issue, we first determined the baseline uptake of a single dose of 800CW-PGN650 in BT474 breast tumors in the absence of chemotherapy and imaged tumors over a 7-day period. As anticipated, the peak T/N ratios were similar among all groups prior to docetaxel treatment, with an average T/N ratio of 3.45 at the 24-hour imaging time point. After 7 days, the same animals were separated into four groups (three animals/group) and given docetaxel (10 mg/kg, IP) at varying times prior to injection of a second dose of 800CW-PGN650 (Figure 6). Tumor NIR images following injection of 800CW-PGN650 were diminished at the 48-hour and 168-hour time points, with average T/N ratios of 2.71 and 1.94, respectively. Immediately following tumor imaging at the 168-hour time point, groups of mice were treated with docetaxel at 72 hours, at 48 hours, at 24 hours, or immediately prior to the second dosing with 800CW-PGN650. Docetaxel injection enhanced the targeting of 800CW-PGN650 in all treatment groups regardless of the timing of chemotherapy injection. The largest difference in the T/N ratio between pre- and postchemotherapy occurred when docetaxel was dosed 24 hours prior to injection of 800CW-PGN650, with a T/N ratio of 6.45 measured 24 hours post-probe injection ($p = .03$).

Discussion

Imaging of exposed PS in a noninvasive manner in cancer and other diseases is a well-recognized marker to monitor disease status, as well as providing confirmation on the responsiveness to therapy.^{16,25-28} PS is exposed in cells in response to activation or cellular stresses and apoptotic or necrotic cells. Exposure of PS in viable tumor ECs is an ideal marker for detection of tumors and measuring a response to therapy because growing tumors require adequate blood supply from functional tumor vasculature.²⁹ Previous studies showed that the majority of PS-positive tumor ECs in vivo are viable, nonapoptotic cells as judged

by TUNEL staining.⁸ Injection of PGN635 in tumor-bearing mice rapidly localizes to tumor ECs and remains on the cell surface for several days because significant internalization of PS does not occur.²³ Although PGN650 is capable of binding to PS located on the internal membrane leaflet of apoptotic or necrotic cells in tumors, a significant portion of PGN650 targets tumor ECs and remains as a stable complex on the cell surface for several days. In this report, we have demonstrated that 800CW-PGN650 effectively targets exposed PS in tumors in mice and enhanced uptake of the probe is consistently detected following administration of chemotherapy. Pretreatment of animals with docetaxel is shown to enhance the targeting of 800CW-PGN650 in each of the tumor systems used in our studies. 800CW-PGN650 binding in tumors was observed to colocalize with CD31⁺ tumor blood vessel endothelial cells in the absence of chemotherapy with enhanced binding to both tumor endothelium and tumor cells in animals treated with docetaxel. These data support previous observations that chemotherapeutic agents, including docetaxel, and irradiation increase the surface exposure of PS in tumors, including both tumor blood vessel ECs and tumor cells.^{8,17,18,30,31}

In previous studies using bavituximab radiolabeled with ⁷⁴As for PET imaging, increased uptake of ⁷⁴As bavituximab was observed in a rat model of prostate cancer, with the peak tumor to liver ratio observed 72 hours postinjection of probe.²¹ Recently, 800CW-PGN650 uptake was demonstrated by NIR optical imaging in a model of rat glioma and irradiation-enhanced probe uptake in tumors.²³ Our study extends recent observations that 800CW-PGN650 can be used to image tumors and detect an enhanced exposure of PS on tumor vasculature in response to chemotherapy. The presence of 800CW-PGN650 probe in tumors for at least 120 hours postinjection indicates that stable PS-β2GPI complexes are formed on the surface of tumor vasculature and are retained in tumors well after clearance of the probe from circulation. These data provide evidence that sufficient targeting is achieved with a F(ab')₂ fragment while minimizing exposure that may contribute to off-target tissue binding or possibly the induction of host immune responses to the probe following multiple injections.

Annexin V has been extensively evaluated as an imaging agent to monitor exposed PS in preclinical and clinical studies as a way to monitor responses to chemotherapy.²⁵ PS and PE are both externalized to the cell surface of stressed or apoptotic cells, including tumor vasculature, and can both be targeted by annexin V.³² Given that PGN650 targets exposed PS and not PE, this raises the possibility that annexin V could be a more sensitive probe to detect phospholipid externalization in tumor vasculature. However, in healthy cells, the asymmetry of PS is more tightly regulated than that of PE due to higher affinity and the rate of PS transported by enzymes, which could explain the higher level of exposed PE during cellular stress^{32,33} and the higher off-target exposure in healthy tissues such as kidney.³⁴ Thus, although annexin V may be more sensitive to detect changes in externalized phospholipids, lower off-target background signals may be achieved by PGN650. An important issue requiring consideration is the timing of PS imaging after chemotherapy treatment. Peak uptake of ^{99m}Tc-annexin V in preclinical tumor models and cancer patients pretreated with chemotherapy has shown greater variability.^{24,25} The inconsistent targeting by annexin V may be attributed to variation with the onset of cellular stresses³⁵ or possibly blocking of cell binding by the release of PS-positive microvesicles into the circulation

following chemotherapy.^{36,37} This variability poses challenges in the use of annexin V because it has a short circulating half-life (less than 10 minutes) and may require multiple injections to target peak PS exposure in response to chemotherapy.¹⁵ To circumvent the problem of short half-life, proposals have been made to either give multiple injections of annexin V³⁵ or modify the protein by pegylation to increase the half-life.³⁸ However, whereas protein modification of annexin V may lead to increased kidney tissue reactivity and toxicity,³⁹ no toxicities were observed in preclinical toxicity studies in rats using PGN650 up to 10 mg/kg and up to 100 mg/kg of the full-length PGN635 IgG following repeated dosing in rats and monkeys (data not shown). The lack of toxicity and off-target reactivity of PGN650 has, in part, provided a basis to initiate a clinical study to evaluate I-124 PGN650 as a PET imaging agent in patients with solid tumors. Thus, PGN650 has advantages over annexin V as a PS-binding imaging agent due to a longer (6 hour) half-life without chemical modification,²³ decreased reactivity and toxicity to normal tissue, and lower potential to elicit host immune responses following multiple injections.

Dual modality imaging using NIR imaging and BLI for preclinical studies is an effective alternative to previously established imaging modalities such as magnetic resonance imaging (MRI), PET, and SPECT. NIR imaging and BLI do not require ionizing radiation or radioactive materials and are powerful tools for noninvasive in vivo imaging of responses to tumors. Although the utility of NIR imaging is established for small-animal tumor studies, the detection of small tumors and metastases in deep tissues in humans may require conjugation of radionuclides to antibodies to maximize the sensitivity of detection. Data obtained in this study indicate that primary human xenografts can be readily detected by 800CW-PGN650 in the absence of chemotherapy; however, the limit of detection of 800CW-PGN650 uptake in tumors was 0.3 mg/kg. This limitation is likely due to several factors, including penetration of NIR signals through tissues and the level of PS exposed on the tumor surface. Conjugation of PGN650 to radionuclides such as ¹²⁴I and ⁶⁴Cu for PET and ¹¹¹In for SPECT will be preferred for clinical studies to accurately image exposed PS in tissues.⁴⁰⁻⁴³

An important consideration when measuring the upregulation of PS exposure is the time interval between dosing of chemotherapy and optimal PS exposure in tumors. In the current study, peak NIR signals from tumors were observed when docetaxel was administered 24 hours prior to injection of 800CW-PGN650 and detection of NIR signals persisted for at least 120 hours following injection of the probe. In human clinical studies, which use lower concentrations of biologic probes, the consistency of tumor uptake will likely be impacted by several variables, including circulating probe half-life, tissue penetration, timing of response to therapy, and the presence of circulating inhibitors to tissue uptake. Given that PGN650 has a circulating half-life of 6 hours,²³ this may provide a larger time frame compared to annexin V (10-minute half-life) to detect responses to therapy in humans. The formation of plasma membrane-derived microparticles or exosomes—which have PS on the surface and are shed from endothelial, tumor, platelet, and immune cells—may inhibit targeting to PS in tumors when the imaging agent is given at low doses.³⁷ Inhibition of tumor uptake of probe by shed microparticles may contribute to variation in uptake of ^{99m}Tc-annexin in tumors of mice following treatment with doxorubicin.²⁴ Clearance of shed microparticles from the circulation following chemotherapy may thus be an important

consideration in accurately measuring the tumor response to chemotherapy using imaging agents that target PS exposure in tumors.

Measurement of enhanced PS exposure in response to therapy has gained greater recognition as a biomarker for developing more effective treatments for cancer. To determine a response to therapy in clinical studies, baseline probe uptake is determined prior to therapy and compared to posttreatment uptake following a second injection of probe. Data from our study demonstrate that the peak T/N ratio of probe uptake following treatment with docetaxel was significantly higher than baseline probe uptake and also occurred 24 hours after docetaxel treatment, with imaging 24 hours after probe injection. These results confirm that repeat administration of PGN650 to detect enhanced PS levels in tumors is feasible and the washout interval between probe administrations can be as short as 1 week. Additionally, using the same approach to detect enhanced 800CW-PGN650 uptake in tumors following chemotherapy, it should be feasible to optimize different chemotherapy regimens and timing for specific tumor types. This optimization may be useful for selecting chemotherapy regimens and tumor types to be used in future clinical studies with bavituximab.

Conclusion

We have shown that 800CW-PGN650 can be used to image tumors and detect enhanced PS exposure in response to chemotherapy. These data support further development of PGN650 as a broad-spectrum tumor imaging agent to detect tumors and to measure their response to different modalities of therapy, including chemotherapy.

Acknowledgments

We thank Anita Kavlie, Affitech (Oslo, Norway) and Kyle Schlunegger, Peregrine Pharmaceuticals, for construction of the PGN635 antibody; Philip Thorpe, University of Texas Southwestern Medical Center; and Steven King, Peregrine Pharmaceuticals, for technical guidance and support.

References

1. Hirsch FR, Franklin WA, Gazdar AF, Bunn PA Jr. Early detection of lung cancer: clinical perspectives of recent advances in biology and radiology. *Clin Cancer Res.* 2001; 7:5–22. [PubMed: 11205917]
2. Holmgren L, O'Reilly MS, Folkman J. Dormancy of micrometastases: balanced proliferation and apoptosis in the presence of angiogenesis suppression. *Nat Med.* 1995; 1:149–53. doi:10.1038/nm0295-149. [PubMed: 7585012]
3. Belhocine T, Steinmetz N, Green A, Rigo P. In vivo imaging of chemotherapy-induced apoptosis in human cancers. *Ann N Y Acad Sci.* 2003; 1010:525–9. [PubMed: 15033784]
4. Williamson P, Schlegel RA. Back and forth: the regulation and function of transbilayer phospholipid movement in eukaryotic cells. *Mol Membr Biol.* 1994; 11:199–216. doi: 10.3109/09687689409160430. [PubMed: 7711830]
5. Balasubramanian K, Schroit AJ. Aminophospholipid asymmetry: a matter of life and death. *Annu Rev Physiol.* 2003; 65:701–34. doi:10.1146/annurev.physiol.65.092101.142459. [PubMed: 12471163]
6. Ran S, Downes A, Thorpe PE. Increased exposure of anionic phospholipids on the surface of tumor blood vessels. *Cancer Res.* 2002; 62:6132–40. [PubMed: 12414638]
7. Ran S, Thorpe PE. Phosphatidylserine is a marker of tumor vasculature and a potential target for cancer imaging and therapy. *Int J Radiat Oncol Biol Phys.* 2002; 54:1479–84. doi:10.1016/S0360-3016(02)03928-7. [PubMed: 12459374]

8. Huang X, Bennett M, Thorpe PE. A monoclonal antibody that binds anionic phospholipids on tumor blood vessels enhances the antitumor effect of docetaxel on human breast tumors in mice. *Cancer Res.* 2005; 65:4408–16. doi:10.1158/0008-5472.CAN-05-0031. [PubMed: 15899833]
9. Stace CL, Ktistakis NT. Phosphatidic acid- and phosphatidylserine-binding proteins. *Biochim Biophys Acta.* 2006; 1761:913–26. [PubMed: 16624617]
10. Burtea C, Laurent S, Lancelot E, et al. Peptidic targeting of phosphatidylserine for the MRI detection of apoptosis in atherosclerotic plaques. *Mol Pharm.* 2009; 6:1903–19. doi:10.1021/mp900106m. [PubMed: 19743879]
11. Igarashi K, Kaneda M, Yamaji A, et al. A novel phosphatidylserine-binding peptide motif defined by an anti-idiotypic monoclonal antibody. Localization of phosphatidylserine-specific binding sites on protein kinase C and phosphatidylserine decarboxylase. *J Biol Chem.* 1995; 270:29075–8. doi:10.1074/jbc.270.49.29075. [PubMed: 7493929]
12. Hanshaw RG, Smith BD. New reagents for phosphatidylserine recognition and detection of apoptosis. *Bioorg Med Chem.* 2005; 13:5035–42. doi:10.1016/j.bmc.2005.04.071. [PubMed: 15914007]
13. Buehler A, Herzog E, Ale A, et al. High resolution tumor targeting in living mice by means of multispectral optoacoustic tomography. *EJNMMI Res.* 2012; 2:14. doi:10.1186/2191-219X-2-14. [PubMed: 22464315]
14. Belhocine TZ, Blankenberg FG. 99 mTc-annexin A5 uptake and imaging to monitor chemosensitivity. *Methods Mol Med.* 2005; 111:363–80. [PubMed: 15911991]
15. Stratton JR, Dewhurst TA, Kasina S, et al. Selective uptake of radiolabeled annexin V on acute porcine left atrial thrombi. *Circulation.* 1995; 92:3113–21. doi:10.1161/01.CIR.92.10.3113. [PubMed: 7586283]
16. Blankenberg FG, Katsikis PD, Tait JF, et al. Imaging of apoptosis (programmed cell death) with 99mTc annexin V. *J Nucl Med.* 1999; 40:184–91. [PubMed: 9935075]
17. Beck AW, Luster TA, Miller AF, et al. Combination of a monoclonal anti-phosphatidylserine antibody with gemcitabine strongly inhibits the growth and metastasis of orthotopic pancreatic tumors in mice. *Int J Cancer.* 2006; 118:2639–43. doi:10.1002/ijc.21684. [PubMed: 16353142]
18. Ran S, He J, Huang X, et al. Antitumor effects of a monoclonal antibody that binds anionic phospholipids on the surface of tumor blood vessels in mice. *Clin Cancer Res.* 2005; 11:1551–62. doi:10.1158/1078-0432.CCR-04-1645. [PubMed: 15746060]
19. Luster TA, He J, Huang X, et al. Plasma protein beta-2-glycoprotein 1 mediates interaction between the anti-tumor monoclonal antibody 3G4 and anionic phospholipids on endothelial cells. *J Biol Chem.* 2006; 281:29863–71. doi:10.1074/jbc.M605252200. [PubMed: 16905548]
20. Gerber DE, Stopeck AT, Wong L, et al. Phase I safety and pharmacokinetic study of baviximab, a chimeric phosphatidyl-serine-targeting monoclonal antibody, in patients with advanced solid tumors. *Clin Cancer Res.* 2011; 17:6888–96. doi:10.1158/1078-0432.CCR-11-1074. [PubMed: 21989064]
21. Jennewein M, Lewis MA, Zhao D, et al. Vascular imaging of solid tumors in rats with a radioactive arsenic-labeled antibody that binds exposed phosphatidylserine. *Clin Cancer Res.* 2008; 14:1377–85. doi:10.1158/1078-0432.CCR-07-1516. [PubMed: 18316558]
22. Yin, Y.; Kavlie, A.; Thorpe, PE. Fully human anti-phosphatidylserine antibody inhibits the growth of prostate cancer in mice; In: *Proceedings for the 100th Annual Meeting of the American Association for Cancer Research*; Denver, CO. 2009;
23. Zhao D, Stafford JH, Zhou H, Thorpe PE. Near-infrared optical imaging of exposed phosphatidylserine in a mouse glioma model. *Transl Oncol.* 2011; 4:355–64. [PubMed: 22191000]
24. Mandl SJ, Mari C, Edinger M, et al. Multi-modality imaging identifies key times for annexin V imaging as an early predictor of therapeutic outcome. *Mol Imaging.* 2004; 3:1–8. doi: 10.1162/153535004773861679. [PubMed: 15142407]
25. Belhocine T, Steinmetz N, Hustinx R, et al. Increased uptake of the apoptosis-imaging agent (99m)Tc recombinant human annexin V in human tumors after one course of chemotherapy as a predictor of tumor response and patient prognosis. *Clin Cancer Res.* 2002; 8:2766–74. [PubMed: 12231515]

26. Kown MH, Strauss HW, Blankenberg FG, et al. In vivo imaging of acute cardiac rejection in human patients using (99m)technetium labeled annexin V. *Am J Transplant*. 2001; 1:270–7. doi: 10.1034/j.1600-6143.2001.001003270.x. [PubMed: 12102261]
27. Ishino S, Kuge Y, Takai N, et al. 99 mTc-annexin A5 for noninvasive characterization of atherosclerotic lesions: imaging and histological studies in myocardial infarction-prone Watanabe heritable hyperlipidemic rabbits. *Eur J Nucl Med Mol Imaging*. 2007; 34:889–99. doi:10.1007/s00259-006-0289-x. [PubMed: 17216472]
28. Narula J, Acio ER, Narula N, et al. Annexin-V imaging for noninvasive detection of cardiac allograft rejection. *Nat Med*. 2001; 7:1347–52. doi:10.1038/nm1201-1347. [PubMed: 11726976]
29. Ingber DE, Madri JA, Folkman J. Endothelial growth factors and extracellular matrix regulate DNA synthesis through modulation of cell and nuclear expansion. *In Vitro Cell Dev Biol*. 1987; 23:387–94. doi:10.1007/BF02620997. [PubMed: 2438264]
30. He J, Luster TA, Thorpe PE. Radiation-enhanced vascular targeting of human lung cancers in mice with a monoclonal antibody that binds anionic phospholipids. *Clin Cancer Res*. 2007; 13:5211–8. doi:10.1158/1078-0432.CCR-07-0793. [PubMed: 17785577]
31. He J, Yin Y, Luster TA, et al. Antiphosphatidylserine antibody combined with irradiation damages tumor blood vessels and induces tumor immunity in a rat model of glioblastoma. *Clin Cancer Res*. 2009; 15:6871–80. doi:10.1158/1078-0432.CCR-09-1499. [PubMed: 19887482]
32. Daleke DL. Regulation of transbilayer plasma membrane phospholipid asymmetry. *J Lipid Res*. 2003; 44:233–42. doi:10.1194/jlr.R200019-JLR200. [PubMed: 12576505]
33. Zachowski A, Favre E, Cribier S, et al. Outside-inside translocation of aminophospholipids in the human erythrocyte membrane is mediated by a specific enzyme. *Biochemistry*. 1986; 25:2585–90. doi:10.1021/bi00357a046. [PubMed: 3013308]
34. Stafford JH, Thorpe PE. Increased exposure of phosphatidylethanolamine on the surface of tumor vascular endothelium. *Neoplasia*. 2011; 13:299–308. [PubMed: 21472134]
35. Blankenberg F. To scan or not to scan, it is a question of timing: technetium-99m-annexin V radionuclide imaging assessment of treatment efficacy after one course of chemotherapy. *Clin Cancer Res*. 2002; 8:2757–8. [PubMed: 12231512]
36. Amin C, Mackman N, Key NS. Microparticles and cancer. *Pathophysiol Haemost Thromb*. 2007; 36:177–83. doi:10.1159/000175155. [PubMed: 19176990]
37. Lechner D, Kollars M, Gleiss A, et al. Chemotherapy-induced thrombin generation via procoagulant endothelial microparticles is independent of tissue factor activity. *J Thromb Haemost*. 2007; 5:2445–52. doi:10.1111/j.1538-7836.2007.02788.x. [PubMed: 17922809]
38. Ke S, Wen X, Wu QP, et al. Imaging taxane-induced tumor apoptosis using PEGylated, 111In-labeled annexin V. *J Nucl Med*. 2004; 45:108–15. [PubMed: 14734682]
39. Kemerink GJ, Liu X, Kieffer D, et al. Safety, biodistribution, and dosimetry of 99mTc-HYNIC-annexin V, a novel human recombinant annexin V for human application. *J Nucl Med*. 2003; 44:947–52. [PubMed: 12791824]
40. Lub-de Hooge MN, Kosterink JG, Perik PJ, et al. Preclinical characterisation of 111In-DTPA-trastuzumab. *Br J Pharmacol*. 2004; 143:99–106. doi:10.1038/sj.bjp.0705915. [PubMed: 15289297]
41. Blankenberg FG, Kalinyak J, Liu L, et al. 99 mTc-HYNIC-annexin V SPECT imaging of acute stroke and its response to neuroprotective therapy with anti-Fas ligand antibody. *Eur J Nucl Med Mol Imaging*. 2006; 33:566–74. doi:10.1007/s00259-005-0046-6. [PubMed: 16477433]
42. Lahorte CM, Vanderheyden JL, Steinmetz N, et al. Apoptosis-detecting radioligands: current state of the art and future perspectives. *Eur J Nucl Med Mol Imaging*. 2004; 31:887–919. doi:10.1007/s00259-004-1555-4. [PubMed: 15138718]
43. Cauchon N, Langlois R, Rousseau JA, et al. PET imaging of apoptosis with (64)Cu-labeled streptavidin following pretargeting of phosphatidylserine with biotinylated annexin-V. *Eur J Nucl Med Mol Imaging*. 2007; 34:247–58. doi:10.1007/s00259-006-0199-y. [PubMed: 17021816]

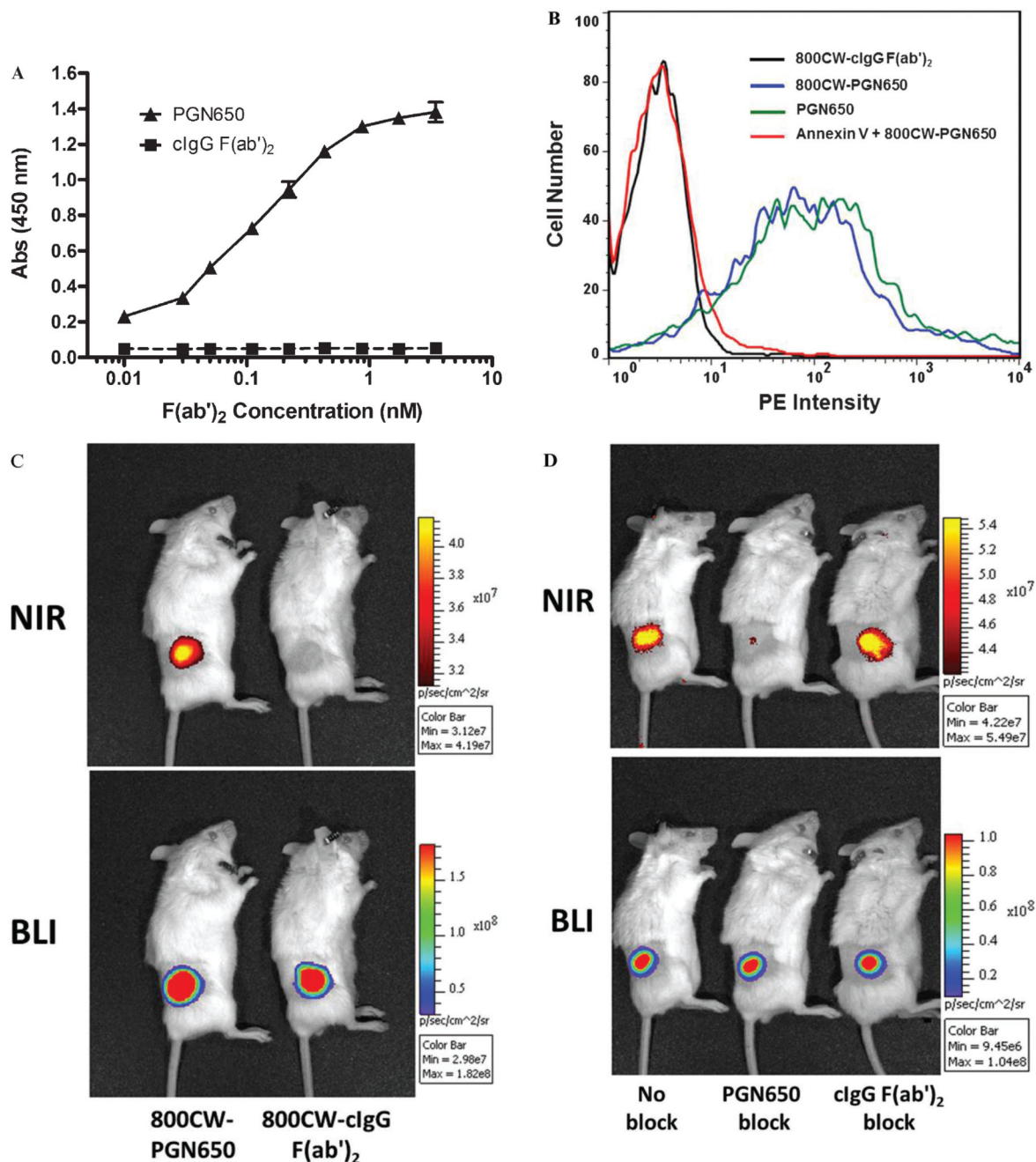


Figure 1.

Targeting of PGN650 to phosphatidylserine (PS). *A*, In vitro targeting of PGN650 to PS on plastic surfaces by ELISA. PS was coated onto a 96-well plastic microplate. Following a blocking step, the primary antibody and control IgG were plated on the assay plate in serial 1:1 dilutions. Wells were washed and incubated with peroxidase-conjugated goat antihuman IgG antibody.

Wells were washed and developed with a peroxidase substrate, and the colorimetric reaction was measured by a spectrophotometric plate reader. Abs = absorbance. *B*, Targeting of PGN650 to PS on cell surface membranes. Jurkat cells treated with etoposide were incubated for 30 minutes with 10 μ g of 800CW-PGN650, 10 μ g of 800CW-PGN650 + 10 μ g of annexin V, 10 μ g of unlabeled PGN650, or 10 μ g of 800CW-cIgG F(ab')₂. Following a second incubation with a 1:100 dilution of

phosphatidylethanolamine (PE)-conjugated goat antihuman F(ab')₂ antibody for 30 minutes, cells were washed and subjected to

FACS analysis. *C*, In vivo targeting of PGN650 to PS in tumors. Mice bearing subcutaneous PC-3luc tumors were injected intravenously with 1 mg/kg of 800CW-PGN650 or 800CW-cIgG F(ab')₂ fragments and imaged 24 hours after injection. Near-infrared (NIR) optical images are shown in the *upper panel* and bioluminescent images (BLIs) are shown in the *lower panel*. *D*, Specific blocking of 800CW-PGN650 targeting in vivo. PC-3luc tumor-bearing animals were untreated or injected with a 50-fold excess of unlabeled PGN650 or unlabeled cIgG F(ab')₂ 10 minutes prior to injection with 1.0 mg/kg of 800CW-PGN650.

NIR optical images are shown in the *upper panel* and BLIs are shown in the *lower panel*.

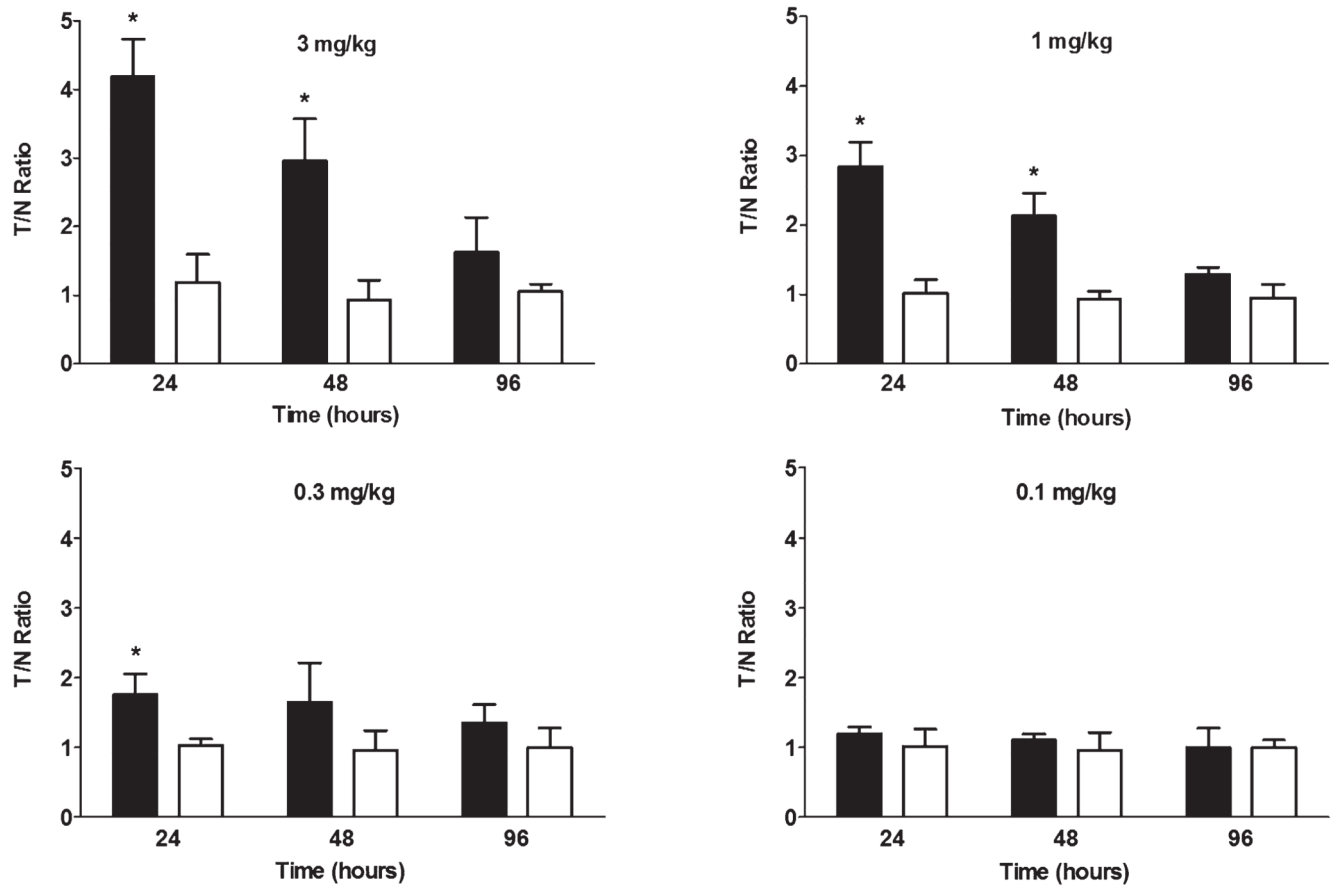


Figure 2.

In vivo dose titration of 800CW-PGN650 binding to tumors. SCID mice bearing subcutaneous PC-3 tumors were injected with 800CW-PGN650 or 800CW-cIgG F(ab')₂ fragments at 0.1, 0.3, 1.0, and 3.0 mg/kg. Near-infrared images corresponding to the bioluminescent image tumor region of interest (ROI) were obtained 24, 48, and 96 hours postinjection. Data are shown as mean \pm SEM of photons/s of the tumor ROI from three animals per treatment group. Statistical analysis between 800CW-PGN650 and 800CW-cIgG F(ab')₂ was performed by t-test; * $p < .05$.

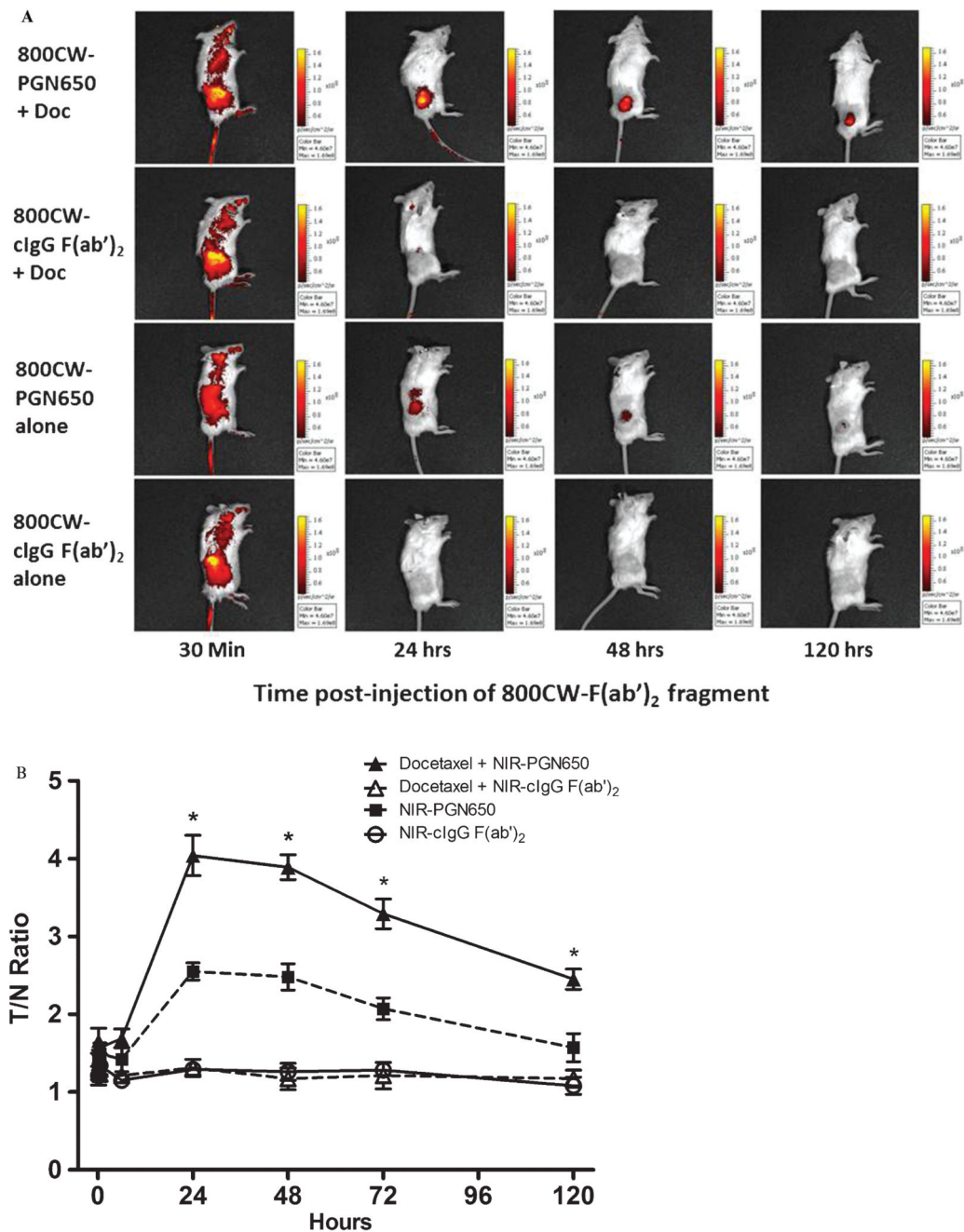


Figure 3.

Chemotherapy enhances uptake of 800CW-PGN650 in human PC3 tumor xenografts. Male SCID mice (four groups of four mice) with subcutaneous PC-3 tumors were injected with or without docetaxel (10 mg/kg, intraperitoneally) 24 hours before administration of 800CW-PGN650 or 800CW-clgG F(ab')₂ (1.0 mg/kg, intravenously). Near-infrared (NIR) imaging was conducted 10 minutes, 30 minutes, 6 hours, 24 hours, 48 hours, 72 hours, and 120 hours following administration of 800CW-labeled antibodies. *A*, Representative whole-body NIR image of a mouse from each treatment group. *B*, Quantified fluorescent tumor/normal tissue ratio of tumor region of interest and comparable normal tissue area. Data are shown as mean \pm SD.

Statistical analysis between 800CW-PGN650 with and without docetaxel was performed by *t*-test; **p* < .05.

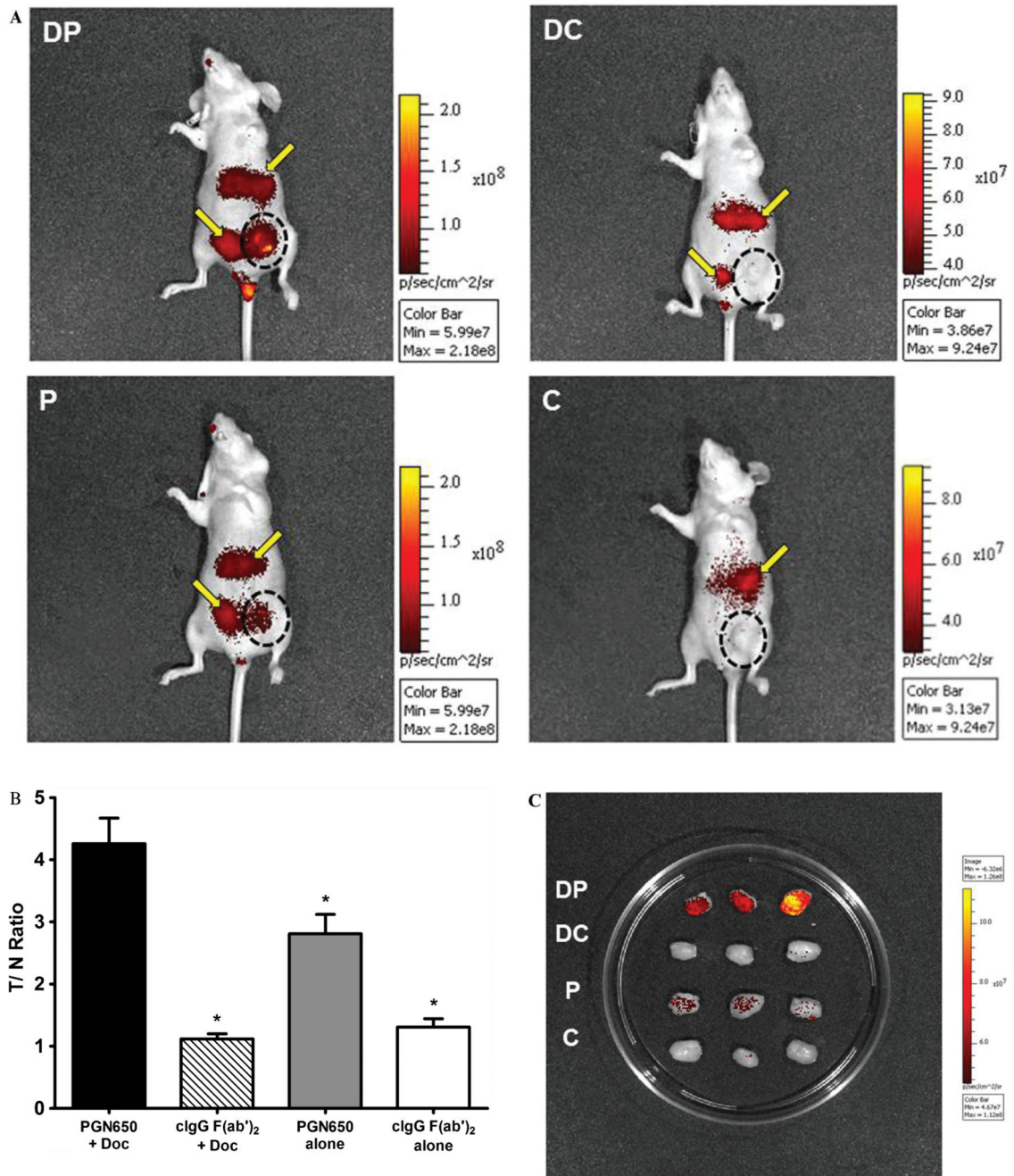


Figure 4.

Docetaxel enhances localization of 800CW-PGN650 in orthotopic BT474 tumors. Female nude mice (four groups of three mice) with orthotopic BT474 breast tumors were injected with docetaxel (10 mg/kg, intraperitoneally) or phosphate-buffered saline 1 day before administration of 800CW-PGN650 or 800CW-cIgG F(ab')₂ (1.0 mg/kg, intravenously). Near-infrared (NIR) imaging was conducted 24 hours following administration of 800CW-labeled antibodies. C = (800CW-cIgG F(ab')₂) alone; DC = docetaxel + 800CW-cIgG F(ab')₂; DP = docetaxel + 800CW-PGN650; P = 800CW-PGN650 alone. A, Representative whole-body NIR image of mice from different treatment groups. The *black dotted circle* indicates the location of the tumor. The *yellow arrow* indicates retention of labeled probes in the liver and bladder. B, Quantified fluorescent tumor to normal tissue ratio at 24

hours. Statistical analysis is shown between docetaxel + 800CW-PGN650 to all remaining groups by *t*-test with statistical significance (*) between groups as $p < .05$. C, NIR image of tumors excised 24 hours following administration of 800CW antibodies.

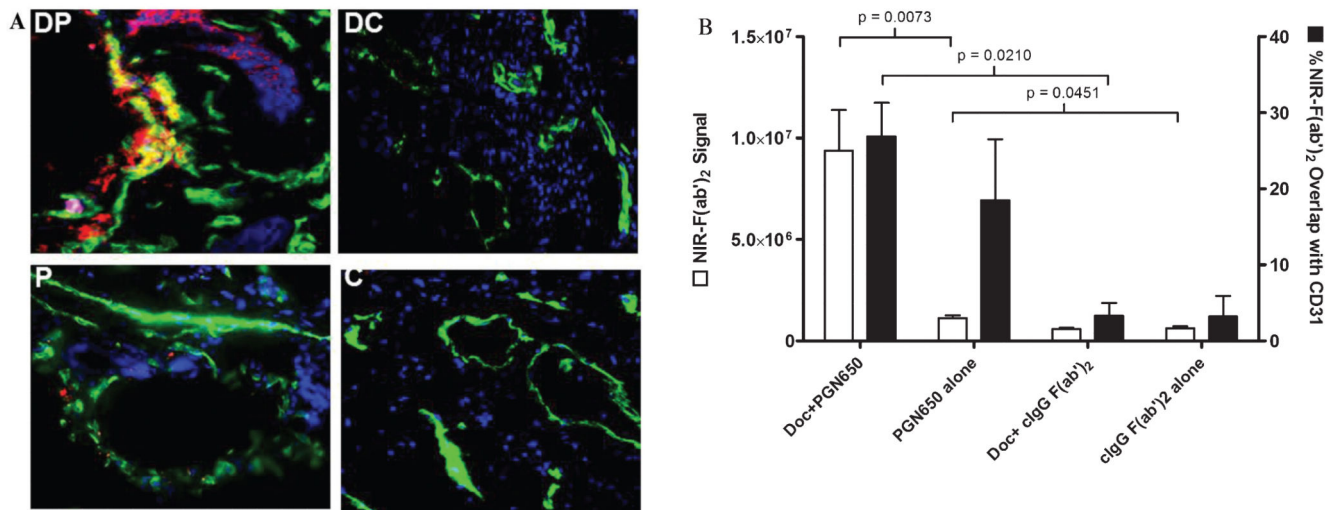


Figure 5.

Fluorescence microscopy of BT474 breast tumors from mice injected with 800CW-PGN650. *A*, Cryosections of tumors shown in Figure 4C were fixed to immobilize the 800CW-labeled F(ab')₂ (red), stained with anti-CD31 Alexa 488 antibodies (green), and nuclei-counterstained with DAPI (blue). Images of representative tissue sections of tumors show colocalization of NIR fragments with vasculature endothelial cells. Overlap of NIR signal with anti-CD31 staining is indicated by yellow color and is most prominent in tumors from animals treated with docetaxel. *C* = (800CW-cIgG F(ab')₂) alone; *DC* = docetaxel + 800CW-cIgG F(ab')₂; *DP* = docetaxel + 800CW-PGN650; *P* = 800CW-PGN650 alone. *B*, Quantitation of NIR signal and overlap with anti-CD31 staining of tissue sections was determined using *MetaMorph* software. The integrated NIR signal (pixel number × intensity) is shown in open bars and % NIR signal overlap with the CD31 signal is indicated with solid bars. Statistical analysis between different groups was performed by *t*-test with statistical significance (*) between groups as $p < .05$.

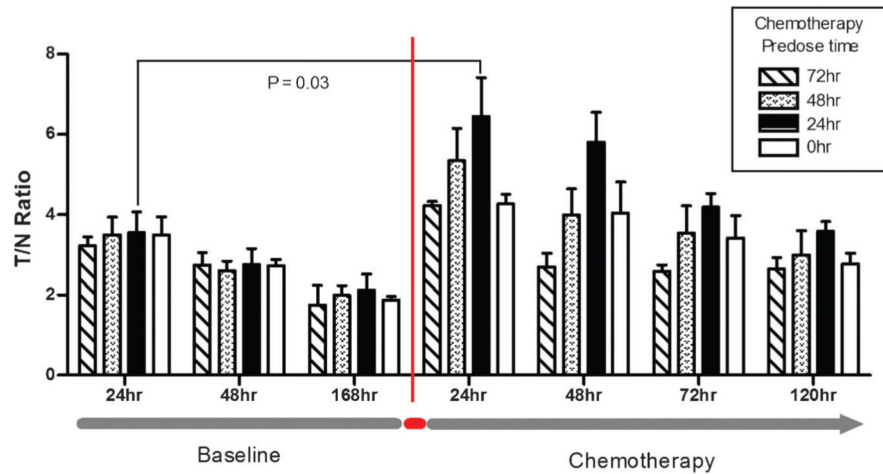


Figure 6.

Repeat administration of PGN650 to measure tumor uptake before and after chemotherapy. Groups of nude mice (four groups of three animals) with orthotopic BT474 breast tumors were given 1.0 mg/kg 800CW-PGN650 by intravenous administration and near-infrared (NIR) tumor region of interest and normal tissue images were collected at 24, 48, and 168 hours. Immediately following the 168-hour image, groups were dosed with docetaxel (10 mg/kg) at 72, 48, 24, and 0 hours prior to a second intravenous injection of 800CW-PGN650 (1 mg/kg). NIR images were collected 24, 48, 72, and 120 hours following the second injection of 800CW-PGN650. Statistical comparison of tumor to normal tissue (T/N) ratios was conducted between the same cohort of animals pre- and postchemotherapy or between cohorts dosed with chemotherapy at different times prior to injection of 800CW-PGN650. Data are represented as the mean \pm SEM. Statistical analysis of T/N ratios pre- and postchemotherapy (docetaxel dosed 24 hours prior to 800CW-PGN650 injection) at the 24-hour imaging time point was determined by paired *t*-test.